Using a Resonant Mechanism to Reduce Energy Consumption in Robotic Arms

M.C. Plooij, M. Wisse
Faculty of Mechanical, Maritime and Material Engineering
Department of BioMechanical Engineering
Delft University of Technology
Delft, The Netherlands

***Abstract*—Conventional robotic arms use motors to accelerate the manipulator. This is energy inefficient when it comes to repetitive tasks. In Europe alone, robotic manipulators use about the same amount of energy as used for the lighting of all households in Portugal. This paper presents an approach to reduce energy consumption in robotic arms by performing its repetitive tasks while moving in a natural mode of the system. The natural mode is created by a resonant spring-loaded mechanism. The performance of the arm with the resonant mechanism is compared to that of the same arm without the resonant mechanism. Simulation studies show that with the resonant mechanism, the robotic arm uses 56% less energy per stroke. Experiments on a prototype show that this is only 14% due to disturbances and friction. With a resonant mechanism, there is an extra energetic cost, because potential energy has to be stored into the spring at startup. This cost is equal to the total energy savings during 8 strokes. Next, there could be an energetic cost to holding the manipulator still outside the equilibrium position. We have designed the resonant mechanism in such a way that this holding cost is negligible for a range of start- and end positions. Note that the resonant mechanism allows the manipulator to freely move to any start- and end-position within a certain range without using latches or other mechanical complications.**

I. Introduction

Currently, there are about 250.000 robotic manipulators operational in Europe. We estimate that their average energy usage is about 2 kW and that they operate for 3000 hours per year. So together they use about 1500 GWh per year, about the same amount as used for the lighting of all households in Portugal [1,2]. Although this number is small compared to other industrial energy consumers, it is large enough to warrant a detailed investigation.

The main reason why robotic manipulators use energy is the use of motors to accelerate the manipulator. In repetitive tasks, the manipulator returns to the same state repetitively. An example of such a task is a pick and place task. Theoretically, such tasks should require no net work, but this requires re-capturing energy when decelerating. We propose to apply a mechanical resonant mechanism, which stores energy during deceleration and releases it during acceleration. For practical applicability, this has to be done while maintaining the freedom to deviate from the natural motions of the resonant mechanism.

The use of natural oscillating motions has already been used in various applications. Akinfiev et al introduced the idea of using nontraditional drives in walking robots [3]. This led to the reduction in energy consumption of 65% in their robot.

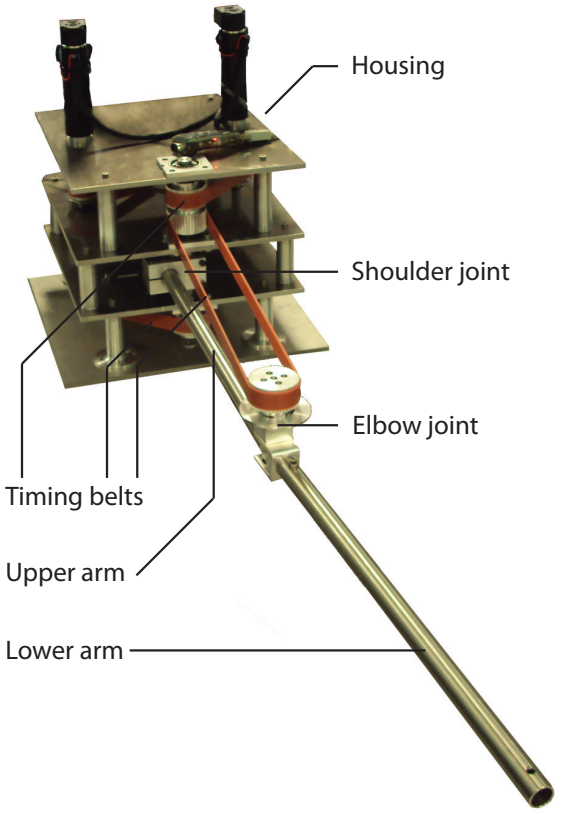

Fig. 1. Prototype of the 2 DOF resonant robotic arm.

However, these nontraditional drives are fully determined so there is little freedom for deviating from the natural motion of the system. Systems with natural motions that do allow for a deviation from the natural motion are compliant resonant mechanisms. These mechanisms have already successfully been used to reduce energy consumption in e.g. toothbrushes [4], compressors [5], shavers [6] and walking robots [7]. The idea of exploiting the natural motions of a system has also been applied on manipulators before. Williamson investigated control strategies for natural oscillating arms [8-11]. However, he applied this on a robot that uses a PD controller with low gains to create oscillating motions, instead of a mechanically oscillating device. The work most strongly related to our study

is that by Akinfiev and others [12-20] who researched mechanically resonant robotic systems and designed mechanisms for those robots. The drawback of these mechanisms is that they lock into place at pre-determined positions. For practical applicability, there is a need for freedom to deviate from the natural motion of the system.

The goal of our study is to implement a resonant mechanism in a robotic arm to reduce its energy consumption, while still being able to deviate from its natural motion using an actuator. The main question in this paper is how much energy the manipulator consumes when it is connected to the resonant mechanism in comparison to when it is not connected to the resonant mechanism.

We show the working principle of the proposed resonant mechanism and we present 3 simulation studies, followed by 2 prototype experiments (see Figure 1) to confirm the results from simulation. Finally, we will conclude that the resonant mechanism we implemented saved energy, while still being practical applicable.

II. Method

We wanted to know the amount of energy we can save by using a resonant mechanism in robotic manipulators with repetitive tasks. Therefore, we performed simulation studies and prototype experiments. Figure 2 shows the 5 configurations we examined. In all 5 configurations, the resonant mechanism was only connected to the shoulder joint.

(a) The working principle is shown in a theoretical model with 1 DOF in the horizontal plane.
(b) The model is made realistic by integrating motor properties and friction in the system.
(c) A second DOF in the horizontal plane is added in the model to show that the principle also works while adding more DOFs to make the system more applicable.
(d) A prototype with 1 DOF is examined to show that the principle works in real life.
(e) A second DOF is added to the prototype to confirm the results from the third simulation.

In all 5 configurations, the energy consumption of the system with the resonant mechanism attached is compared to that of the same system with the resonant mechanism detached.

A. Measurements

We took 3 different types of measurements on the energy consumption of a resonant robotic arm:

- **The amount of energy consumed per stroke.** This is the energy that is needed to move from one operating position of the system to the other. We assumed that negative work by the motor is lost, so that all energy that is re-captured, is re-captured by the resonant mechanism. We compared this value between the situations with and without the resonant mechanism attached. In resp. simulation and prototype experiments we calculated this as follows:

$$E = \sum_{t=0}^{t_s} \max\left(T_{\mathrm{m}}(t) \cdot \dot{\theta}_{\mathrm{m}}(t) + R \cdot \left(\frac{T_{\mathrm{m}}(t)}{K_{\mathrm{t}}}\right)^2; 0\right) \cdot \Delta t$$

$$E = \sum_{t=0}^{t_{\mathrm{s}}} \max(U(t) \cdot I(t); 0) \cdot \Delta t$$

  Where $\dot{\theta}_{\mathrm{m}}$ is the angular speed of the motor, R is the terminal resistance of the motor, K_{t} is the torque constant of the motor, T_{m} is the torque of the motor, U is the voltage on the motor, I is the current through the motor, t_{s} if the time per stroke and Δt is the sampling time, which is 0.0005 seconds in simulation and about 0.005 seconds in the prototype. This calculation neglects self inductance, because the terminal inductances of electromotors in applications like ours, are typically small.
- **The starting up energy.** This is the energy that is needed to put potential energy into the resonant mechanism at the start. This energy is only needed when the resonant mechanism is attached. In both simulation and prototype experiments, this is calculated by looking at the energy consumption while moving the system to its operational position.
  We also calculated the breakeven point, which is the starting up energy divided by the net energy savings per stroke.
- **The standing still energy.** This is the energy needed when the motors are holding the system in place at 0.1 rad outside an equilibrium position of the resonant mechanism. To make it comparable with the amount of energy consumed per stroke, we quantified this as the energy consumed while standing still for half of the time per stroke. In resp. simulation and prototype experiments we calculate this as follows:

$$E = R \cdot \left(\frac{T_{\mathrm{m}}}{K_{\mathrm{t}}}\right)^2 \cdot \frac{t_{\mathrm{s}}}{2}$$

$$E = U \cdot I \cdot \frac{t_{\mathrm{s}}}{2}$$

  where t_{s} is the time per stroke.

III. Resonant Mechanism

Every oscillating mechanical system has a characteristic. In our case, this is the potential energy stored in the spring as a function of the rotation of the shoulder joint (Figure 2c). The torque of the system is related to the potential energy by:

$$T = \frac{dP}{d\theta}$$

Where P is the potential energy stored in the system and θ is the angular displacement. There are 4 requirements on the characteristic of a resonant robotic arm with a repetitive task. These are also indicated in Figure 4.

A. **The resonant mechanism should not counteract the repetitive task.** This means that when the system

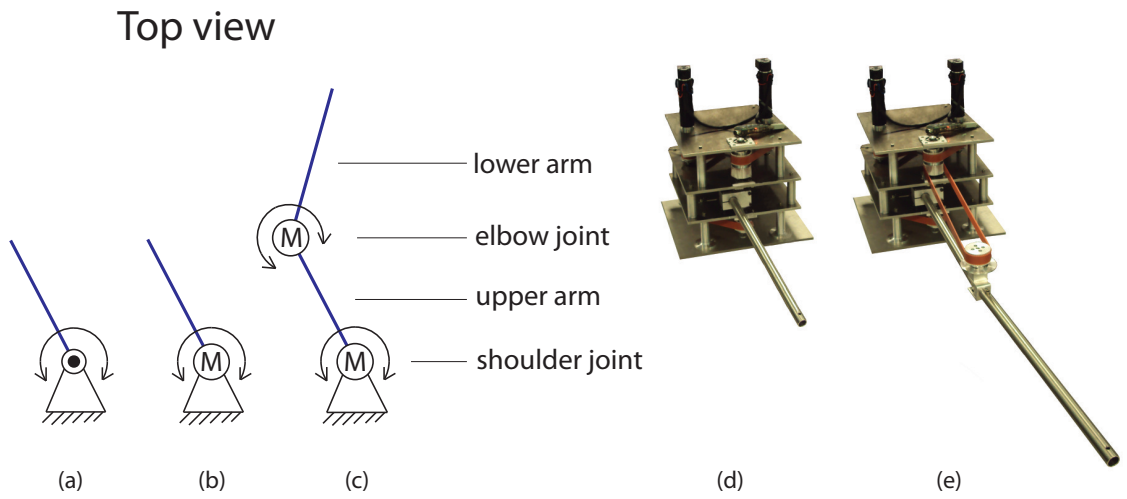

Fig. 2. The 5 configurations that are studied, with 3 top views of the simulations and 2 3D views of the prototype. a) A theoretical model with 1 DOF. Copper losses in the motor and friction are neglected. b) A realistic 1 DOF model with friction and copper losses. c) A realistic 2 DOF model with friction and copper losses. d) A 1 DOF prototype to confirm the results from simulation b. e) A 2 DOF prototype to confirm the results from simulation c. The second DOF is actuated by a motor at the base. The torques are transferred through a timing belt.

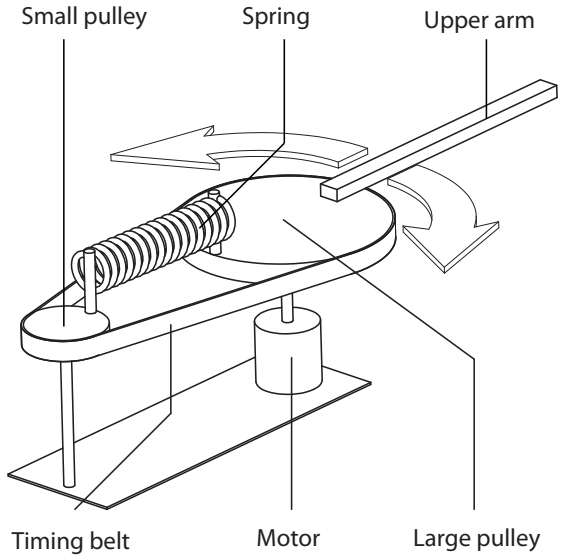

Fig. 3. The concept of the resonant mechanism. The upper arm is connected to the large pulley. This pulley is connected to the small pulley through a timing belt and a spring. The ratio between the diameters of the pulleys and the spring properties determine the characteristic of the resonant mechanism.

is at an operating position, the motor should not have to counteract the resonant mechanism to keep the manipulator in place. Therefore, the derivative of the potential energy as function of the rotation of the shoulder joint should be low around the operating positions. This means that there is no hardly any torque about the joint.

B. **The resonant mechanism should always provide motions from one operating position to the other.** The operating area is the area between the operating positions. Outside the operating area, the resonant mechanism has to provide a torque towards the operating area. Therefore, the potential energy should increase outside the operating area.

C. **The characteristic between the operating positions should be such that the system can make fast motions.** This means a high and fast drop in potential energy between the operating positions. This means a that there is a torque towards the midpoint.

D. **D. In between the operating positions, there should be a point where the potential energy reaches a minimum and the kinetic energy reaches a maximum. This point is called the midpoint**

Linear spring mechanisms do not meet requirement A. Therefore, we propose the resonant mechanism as shown in Figure 3, which has two equilibrium positions at the operating positions. This has the advantage of being energy efficient while still being applicable, because the system can stand still in a range around its operating positions. The working principle of this mechanism is shown in Figure 4. This mechanism is inspired by the work of Babitsky [16].

IV. Simulation Studies

The simulations are modeled in MATLAB. Table I shows the parameters of the simulations. In all studies, the performance of the arm with the resonant mechanism attached is compared to the performance of the arm without the resonant mechanism attached. After results of the theoretical simulation with 1 DOF, we will verify the robustness of the system (how the choice of the speed, the displacement and the mass influence the results).

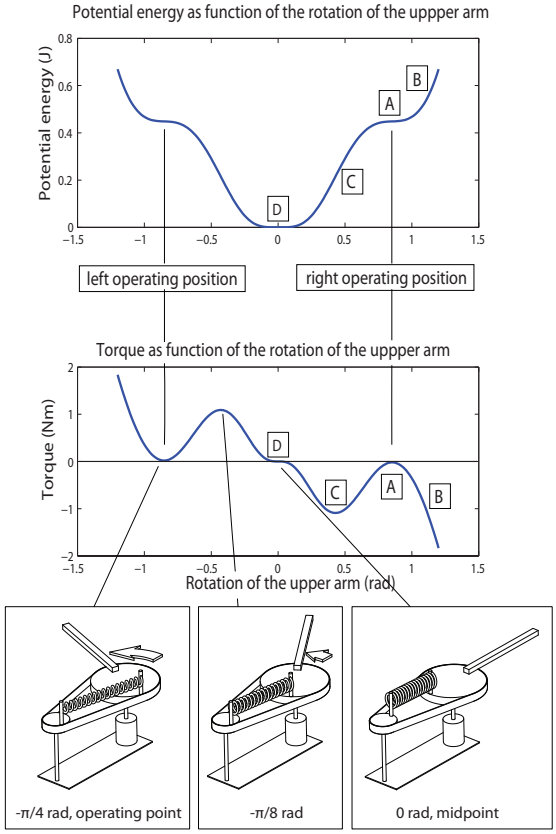

Fig. 4. A visualization of the working principle of the resonant mechanism. The first plot shows the potential energy in the system as function of the rotation of the upper arm. [A], [B], [C] and [D] represent the requirements on the characteristic of the arm. [A]: At the operating position the derivative of the potential energy is equal to 0 J/rad. This means that there is no net. torque. [B]: Outside the operating area, the potential energy increases. This means that there is a torque towards the operating area. [C]: in between the operating positions, the potential energy decreases fast. This means that there is a torque towards the midpoint (D). [D]: At the midpoint, the potential energy has a minimum and the kinetic energy has a maximum. The movement of the arm and the resonant mechanism are visualized at the bottom. When the upper arm reaches an angle of $\pi/4$ rad, the small pulley has rotated for about 4.2 rad and the connection between the spring and the small pulley is moving towards the large pulley, with the same speed as the connection between the spring and the large pulley. This means that with a virtual small rotation of the arm, no extra energy is stored in the system, so the slope of the potential energy graph is horizontal.

TABLE I
MODEL PARAMETERS OF THE SIMULATION AND REQUIREMENTS ON THE STROKE.

Parameter	Symbol	Value
Length of arm	l	0.4 m
Inertia	I	0.2 kg m^2
Spring Stiffness	K	150 N/m
Initial length of spring	l_0	15 cm
Radius of large pulley	r_1	15 cm
Radius of small pulley	r_2	2.8 cm
Friction constant	c	0.02 Nms/rad
Time per stroke	t	1.6 s
Rotation per stroke	θ	1.45 rad

A. A Theoretical 1 DOF Model

Let us first analyze a simple version of this system with 1 DOF, (see Figure 2a) to investigate the energy cost to accelerating the arm itself. We assume that there is no friction and that an ideal motor drives the system. This implies that there are no gearbox losses and the motor has no inertia and no electrical resistance. We assume that negative work by the motor is lost. This leaves us with 1 equation of motion:

$$T + M = I \cdot \ddot{\theta}$$

Where T is the torque applied by the motor, M is the moment due to the resonant mechanism, I is the inertia of the arm and θ is the angle of the arm. The potential energy E_{P} in the resonant mechanism is equal to:

$$E_{\mathrm{P}} = \frac{1}{2} k \cdot x^2$$

with

$$x = \sqrt{\left(r_2 \sin\frac{\theta \cdot r_1}{r_2} - r_1 \sin\theta\right)^2 + \left(r_1 + l_0 + r_2 - r_1\cos\theta - r_2\cos\frac{\theta \cdot r_1}{r_2}\right)^2} - l_0$$

Where k is the spring stiffness, r_1 is the radius of the large pulley, r_2 is the radius of the small pulley and l_0 is the initial length of the spring. From this, we know the moment M about the joint due to the resonant mechanism. The power consumption P of the motor is equal to:

$$P = T \cdot \dot{\theta}$$

When the resonant mechanism is not attached, the motor drives the system with a feed-forward torque profile that is most efficient for the task. With this theoretical model, all the energy consumed by the motor is converted into kinetic energy. This means that the total energy consumed per stroke is equal to the maximum of the kinetic energy during the stroke. Given a certain rotation and time per stoke, this means that we have to accelerate as fast as possible at the start. Theoretically, this is an infinitely high torque during an infinitely small amount of time. Of course, this is totally irrealistic.

When the resonant mechanism is attached, the arm can move in the natural motion of the system, where all potential energy is transferred into kinetic energy during acceleration. During deceleration, the kinetic energy is transferred into potential energy again. Since there is no friction, the motor does not consume any energy.

Figure 5 shows the phase plot, the position plot and the energy plot of the motions in both situations.

Results

A comparison between the robotic arm with and without the resonant mechanism is shown in Table II. From this, we can conclude that the system consumes no energy when the

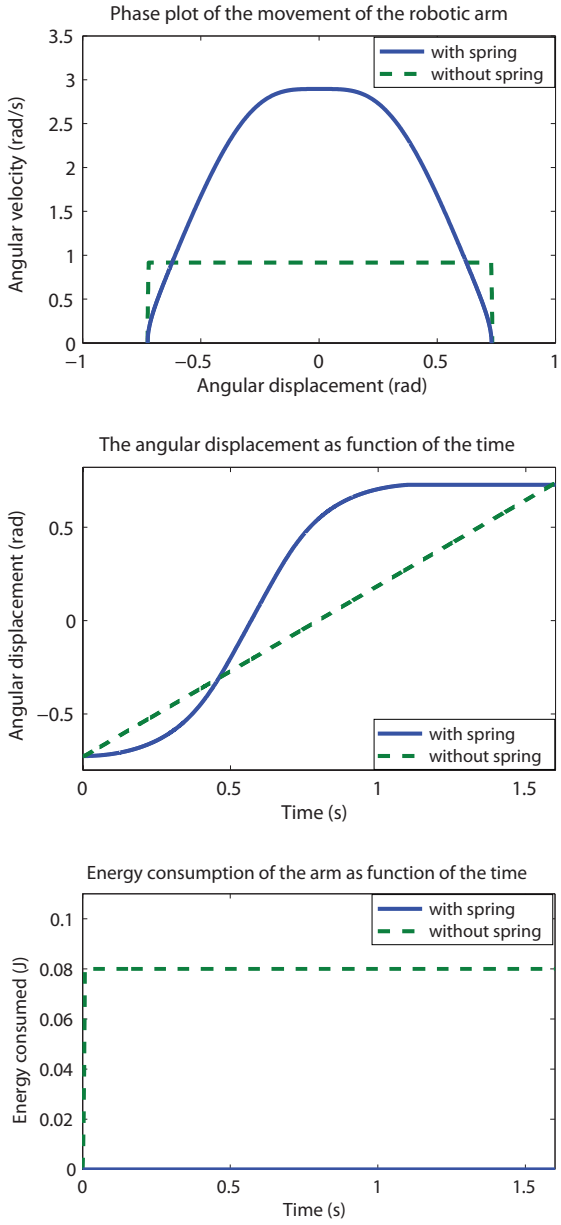

Fig. 5. a) The angular displacement of the arm as function during one stroke. b) Phase plot of the movement of the arm with and without the resonant mechanism attached. c) The accumulated energy that is consumed by the arm as function during one stroke. Plot c shows that all energy is consumed during the acceleration of the system and no energy is re-captured during deceleration.

TABLE II
PERFORMANCE OF THE SIMPLE MODEL OF THE ROBOTIC ARM WITH AND WITHOUT THE RESONANT MECHANISM ATTACHED.

Measurement	With spring	Without spring
Energy per stroke (J)	0.000	0.080
Starting up energy (J)	0.856	0.000
Standing still energy (J)	0.000	0.000

resonant mechanism is attached. The breakeven point is at 24 strokes and the standing still energy is 0 J.

TABLE III
THE ENERGY CONSUMPTION PER STROKE WHEN REQUIRED SPEED, THE ANGULAR DISPLACEMENT AND THE MASS ARE INCREASED WITH 10%.

Changing parameter	Energy per stroke with spring (J)	Energy per stroke without spring (J)	Energy savings
10 % Faster	0.002	0.105	98%
10 % More displacement	0.0.020	0.105	81%
10 % Additional payload	0.001	0.088	99%

Robustness

We will now verify how the choice of the speed, the displacement and the mass influence the results. There are two main questions when it comes to robustness of the concept. How much energy does it cost when speeds, angular displacements and additional payload are varied with the same model parameters? And does the concept still work when it is scaled?

Variation of the requirements

Table I shows the requirements for the speed, the angular displacement and the mass that were arbitrarily chosen for the simulation. The parameters (e.g. spring stiffness) are optimized for these requirements. We now want to know how this system performs when it has to operate with other conditions. Therefore, we evaluate the performance of the system when we decrease the time per stroke, increase the mass of the arm or increase the rotation per stroke.

Table III shows the energy consumption of the arm with and without the resonant mechanism attached, when the parameters are changed with 10%. From this, we can conclude that the system is most sensitive to an increase in angular displacement. This is because the motor has to put extra energy into the spring to get an extra displacement. Therefore, only 81% energy is saved. The system is not influenced by an increase in speed or additional payload, because the spring contains enough energy to deal with these increases. When these parameters are increased with an order of magnitude of 100%, the performance of the system will start to decrease, but the system will still use less energy when the resonant mechanism is attached.

Scaling

When all dimensions are scaled with a factor f, the mass moment of inertia of the system scales with a factor f^5:

$$I = c \cdot m \cdot l^2$$

Where I is the mass moment of inertia, c is a constant which depends on the geometry, m is the mass, which scales with a factor f^3 and l is a measurement for the size of the geometry, which scales with a factor f.

As a result of this scaling, the required kinetic energy in the system also scales with a factor f^5. Therefore, the maximum potential energy in the spring should also scale with a factor

f^5. The potential energy is equal to

$$E_{\mathrm{P}} = \frac{1}{2}kx^2$$

Where x scales with a factor f. Therefore, k should scale quadratically with the scaling of the design to keep the same dynamic behavior:

$$k_{\mathrm{new}} = f^2 \cdot k_{\mathrm{old}}$$

Where k_{new} is the required spring stiffness in the scaled design and k_{old} is the spring stiffness in the unscaled design. This means that when a system is scaled with a factor 2, the spring stiffness should be 4 times the original spring stiffness to keep the same dynamic behavior.

B. A Realistic 1 DOF Model

The previous paragraphs showed that the concept works well for an idealized system with no friction. In this section we will examine what happens when we add the motor, gearbox and friction to the system (see Figure 2b). The motor specifications are based on a Maxon RE30 60W motor with a gearbox ratio of 66:1. An additional ratio of 3:1 is provided by timing belts. Why this motor and gearbox are selected is explained in section V. The motor dynamics are implemented in the model as:

$$I_{\mathrm{tot}} = I_{\mathrm{l}} + I_{\mathrm{m}} \cdot n^2$$
$$T_{\mathrm{l}} = T_{\mathrm{m}} \cdot \eta \cdot n - T_{\mathrm{f}}$$

Where I_{m} is the inertia of the rotor, I_{l} is the inertia of the load, η is the efficiency of the gearbox, n is the gearbox ratio times the transfer ratio of the timing belts, T_{m} is the torque provided by the motor, which is limited, T_{l} is the required torque on the load and T_{f} is the friction torque. We assumed pure viscous friction, which is equal to:

$$T_{\mathrm{f}} = -c \cdot \dot{\theta}$$

Where c is the viscous friction constant and $\dot{\theta}$ is the angular speed of the joint. The power consumption P of the motor is equal to:

$$P = \max\left(T_{\mathrm{m}} \cdot \dot{\theta}_{\mathrm{m}} + R \cdot \left(\frac{T_{\mathrm{m}}}{K_{\mathrm{t}}}\right)^2 ; 0\right)$$

Where $\dot{\theta}$ is the angular speed of the motor, R is the terminal resistance of the motor and K_{t} is the torque constant of the motor.

When the resonant mechanism is detached, the system is driven by a combination of feed-forward and feedback. A maximum torque is applied while accelerating, until the system reaches a speed that is high enough to reach the target position in time in the theoretical model. Then, the motor keeps the system on a constant speed, until the target is almost reached. The system is then decelerated using maximum torque.

When the resonant mechanism is attached, the motor has to overcome the friction. Therefore, a PD energy controller is applied to control the sum of the kinetic and spring energy:

$$T = K_{\mathrm{p}} \cdot (E_{\mathrm{ref}} - E_{\mathrm{state}}) + K_{\mathrm{d}} \cdot \frac{d(E_{\mathrm{ref}} - E_{\mathrm{state}})}{dt}$$

where K_{p} is the proportional gain, K_{d} is the derivative gain, E_{ref} is the potential energy in the resonant mechanism at operating positions and E_{state} is the sum of the potential and kinetic energy in the system.

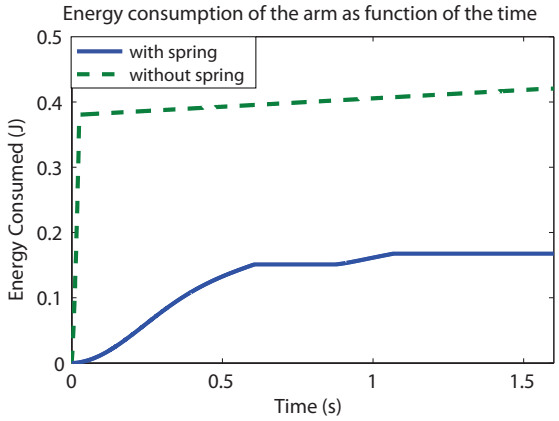

Fig. 6. The accumulated energy consumed in simulation by the 1 DOF robotic arm during 1 stroke. Without the spring, the system consumed most of its energy at the start. After that, the motors only have to compensate for friction. With the spring, the motor consumes most of its energy while accelerating, because the motor has to keep up with the natural motion of the resonant mechanism.

TABLE IV
PERFORMANCE OF THE REALISTIC MODEL OF THE ROBOTIC ARM WITH AND WITHOUT THE RESONANT MECHANISM ATTACHED.

Measurement	With spring	Without spring
Energy per stroke (J)	0.168	0.420
Starting up energy (J)	1.439	0.000
Standing still energy (J)	0.007	0.000

Results

The energy consumption of the system with and without the resonant mechanism is shown in Figure 6. A comparison between the robotic arm with and without the resonant mechanism is shown in Table IV. From this, we can conclude that the system consumes 60% less energy when the resonant mechanism is attached. This is significantly less than the result from the theoretical model because of the losses due to friction, the added inertia of the motor and copper losses. The breakeven point is at 6 strokes and the standing still energy is 0.007 J, which is negligible.

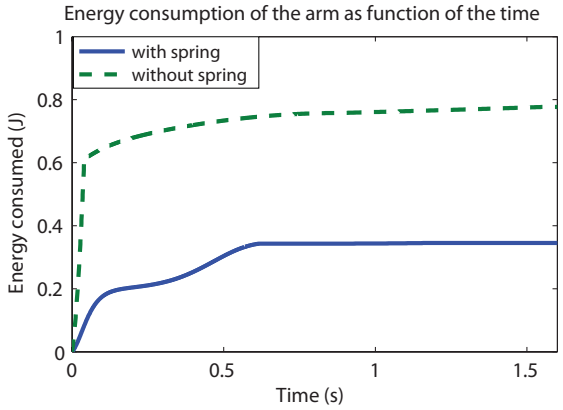

Fig. 7. The accumulated energy consumed in simulation by the 2 DOF robotic arm during 1 stroke. The energy consumptions of both motors are added in this graph. Without the spring, the system consumed most of its energy at the start. After that, the motors only have to compensate for friction. With the spring, the motor consumes most of its energy while accelerating, because the motor has to keep up with the natural motion of the resonant mechanism.

TABLE V
PERFORMANCE OF THE REALISTIC MODEL OF THE 2 DOF ROBOTIC ARM WITH AND WITHOUT THE RESONANT MECHANISM ATTACHED.

Measurement	With spring	Without spring
Energy per stroke (J)	0.345	0.777
Starting up energy (J)	1.787	0.000
Standing still energy (J)	0.007	0.000

C. A Realistic 2 DOF Model

For practical applicability, the system needs at least one more DOF. Therefore, we add a second DOF in the horizontal plane (Figure 2c). This second DOF is actuated by the same type of motor from the base, through a parallel mechanism, which is created by a timing belt. The controllers for the first DOF are still the same as the ones in the realistic simulation with 1 DOF. The second DOF is controlled by a PD position controller.

Results

The energy consumption of the system with and without the resonant mechanism is shown in Figure 7. A comparison between the robotic arm with and without the resonant mechanism is shown in Table V. From this, we can conclude that the system consumes 56% less energy when the resonant mechanism is attached, the breakeven point is at 5 strokes and the standing still energy is 0.007 J, which is negligible.

V. EXPERIMENTS AND RESULTS

A. 1 DOF Dimensional Design

The 1 DOF implemented mechanism as shown in Figure 8 is slightly different from the conceptual design in Figure 3. A picture of the prototype (with 2 DOFs) can be seen in Figure 1. The DOF in the horizontal plane is created by a 18x1.5mm stainless steel tube, connected with a joint. The motor is placed on a housing, which also contains the resonant mechanism. AT3-gen III 16mm timing belts were used to transfer torques

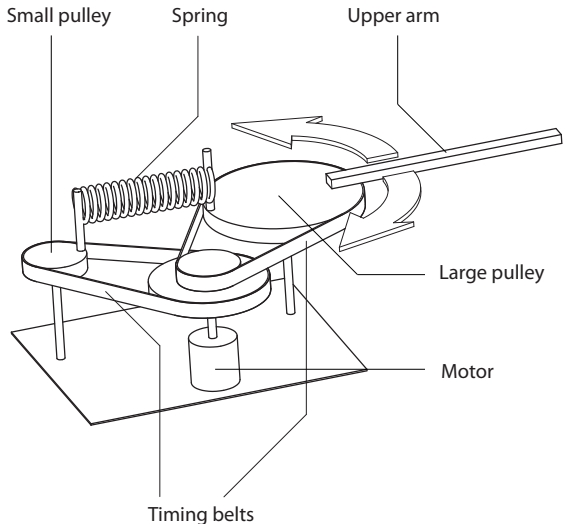

Fig. 8. A schematic picture of the practical implementation of the resonant mechanism in the 1 DOF prototype. In comparison to the concept, an extra timing belt and 2 extra pulleys were added because it was easier to drive the large pulley through a timing belt instead of directly connecting it to the motor and it was hard to get the right transfer ratio between the large and the small pulley.

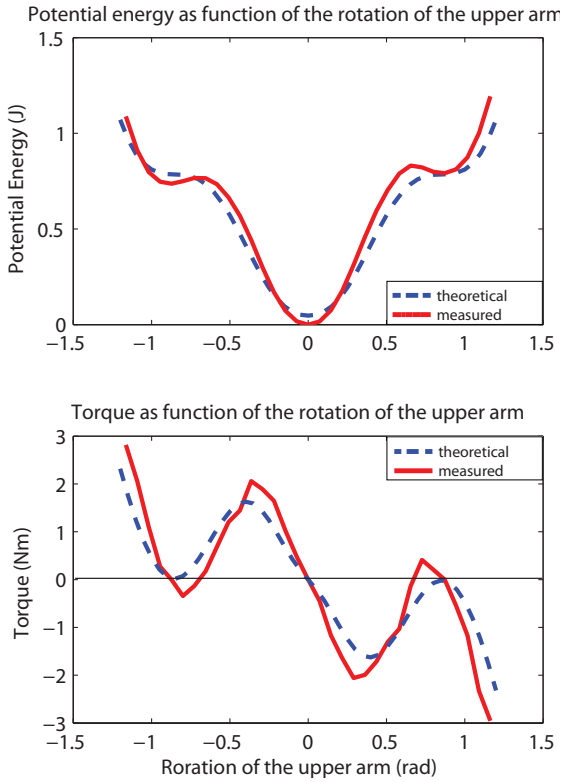

Fig. 9. The characteristic of the resonant mechanism. The solid line is obtained by measurements. The dotted line is the theoretical characteristic.

within the housing. The motor was selected after simulating the system without the resonant mechanism in MATLAB. The joint is actuated by a Maxon 60W RE30 motor with a gearbox

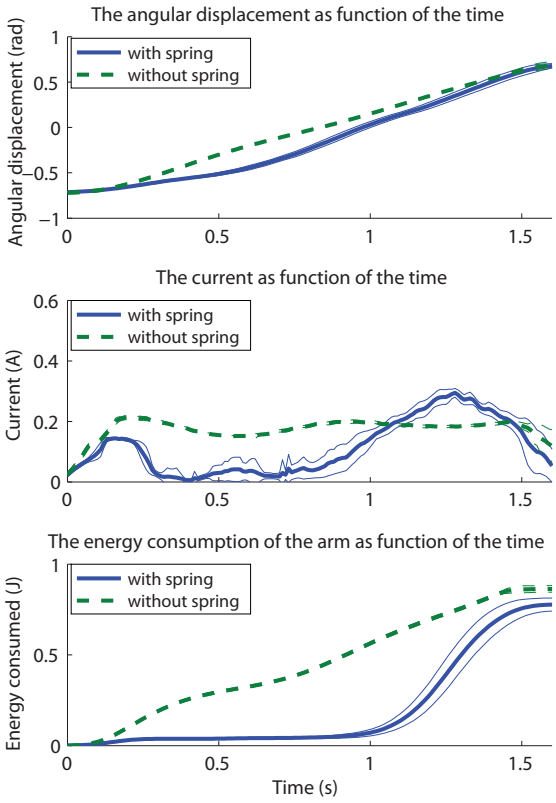

Fig. 10. The data of the 1 DOF prototype with and without the spring. The thick lines show the mean over different strokes, the thin lines show the standard deviations.

TABLE VI
DESIGN PARAMETERS OF THE RESONANT ROBOTIC ARM AND REQUIREMENTS ON THE STROKE

Parameter	Symbol	Value
Length of arm	l	0.4 m
Added mass at end point	M	1 kg
Spring Stiffness	K	150 N/m
Initial length of spring	l_0	10 cm
Radius of large pulley	r_1	10 cm
Radius of small pulley	r_2	2 cm
First transfer ratio	R_1	1:1.8
Second transfer ratio	R_2	1:3
Time per stroke	t	1.6 s
Rotation per stroke	θ	1.45 rad

TABLE VII
PERFORMANCE OF THE 1 DOF PROTOTYPE WITH AND WITHOUT THE RESONANT MECHANISM ATTACHED.

Measurement	With spring	Without spring
Energy per stroke (J)	0.78	0.87
Starting up energy (J)	1.04	0.00
Standing still energy (J)	0.00	0.00

ratio of 66:1. The timing belts provide an additional transfer ratio of 3:1. The design parameters are shown in Table VI. The measured characteristic of the resonant mechanism is compared to the theoretical characteristic in Figure 9.

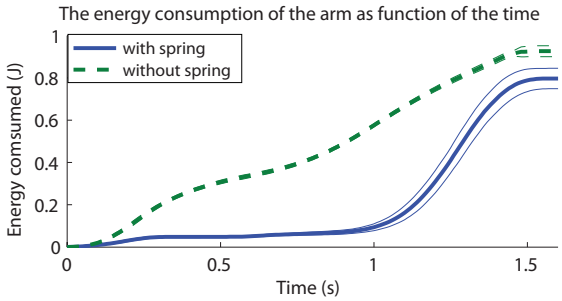

Fig. 11. The accumulated energy consumption of the 2 DOF prototype with and without the spring. The thick lines show the mean over different strokes, the thin lines show the standard deviations.

TABLE VIII
DESIGN PARAMETERS OF THE SECOND DOF OF THE RESONANT ROBOTIC ARM.

Parameter	Symbol	Value
Length of the lower arm	l_1	0.4 m
Mass of the arm	m	0.5 kg
Added mass at end point	M	1 kg

TABLE IX
PERFORMANCE OF THE 2 DOF PROTOTYPE WITH AND WITHOUT THE RESONANT MECHANISM ATTACHED.

Measurement	With spring	Without spring
Energy per stroke (J)	0.80	0.93
Starting up energy (J)	1.03	0.00
Standing still energy (J)	0.00	0.00

Results

The data of the movements of the prototype with 1 DOF is shown in Figure 10. A comparison between the performance of the prototype with 1 DOF is shown in Table VII. From this, we can conclude that with 1 DOF the system consumes 10% less energy when the resonant mechanism is attached, the breakeven point is at 12 strokes and the standing still energy is 0 J.

B. 2 DOF Dimensional Design

We add a second DOF to make the system more applicable. A picture of the 2 DOF prototype can be seen in Figure 1. The second DOF is created by a 18x1.5mm stainless steel tube, connected with the elbow joint. This elbow joint is actuated by a motor in the housing through a timing belt, which creates a parallel mechanism. The extra design parameters are shown in Table VIII.

Results

The energy consumption of the prototype with 2 DOFs is shown in Figure 11. A comparison between the performance of the prototype with 2 DOFs with and without the resonant mechanism is shown in Table IX. From Table IX, we can conclude that with 2 DOFs the system consumes 14% less energy when the resonant mechanism is attached, the breakeven point is at 8 strokes and the standing still energy is 0 J.

VI. Discussion

Without the resonant mechanism, the system works as a conventional arm. Simulations show that it uses 56% less energy per stroke than conventional manipulators. Prototype experiments confirm that the resonant mechanism saves energy, although this was only 14%. Furthermore, experiments show that the breakeven point is at 8 strokes and the standing still energy is negligible.

Energy and friction

The main difference between the simulation models and the prototype is the frictional behavior. In simulations we assumed pure dynamic friction, where in the prototype (and mainly in the gearbox) also static friction occurred. Next, the spring was not connected to the pulleys with bearings. Therefore, the resonant mechanism caused disturbances while moving. These disturbances can be seen in Figure 10b, where the standard deviation of the current is higher in the system with the spring attached. From Table VII and IX we can conclude that the system saves more energy with 2 DOFs than with 1 DOF. This can be explained by the higher inertia of the system which reduces the influence of disturbances from the spring on the system.

Energy and controller

In Figure 10c and 11 we can see that the system indeed profits from the spring. The energy consumption at the start of the movement is significantly less when the spring is attached. However, the system doesnt seem to be able to re-capture all energy efficiently. Therefore, the energy consumption is high between t = 1 s and t = 1.5 s. A better controller should be able to re-capture more energy.

Resonant mechanism

In Figure 9 the measured characteristic is compared to the theoretical characteristic. From this, we can conclude that the characteristic of the implemented mechanism is similar to the desired characteristic. However, there is 1 relevant difference. We can see that instead of 1 sTable and 2 unsTable equilibrium points, the prototype has 3 sTable equilibrium points. This is not optimal because when the system is at a sTable operating position, it has to overcome an energy barrier to move to the other operating position. This is energy inefficient.

Current measurements

The current was measured with a sensor on the controller board, which was calibrated. This sensor turned out to be inaccurate below 0.1 A. Therefore, below this level an estimation of the current was made based on the voltage on the motor. Since the current was mainly low with the spring attached, this correction increased the value of the energy consumption of the system with the spring attached.

Future works

This paper presents a resonant robotic arm with a characteristic, based on the movements the system should make according to our ideas. This doesnt guarantee that this is the optimal characteristic given a certain task. Therefore the resonant mechanism has to be optimized.

In this paper, a PD energy controller was implemented that keeps the sum of the kinetic and the potential energy constant. We think that more energy can be saved using an optimal controller and advice to use reinforcement-learning algorithms. These algorithms can also learn how to do different kinds of tasks.

The current sensor on the controller board was not accurate at currents below 0.1 A. This sensor has to be replaced with a more accurate one.

To make the system more applicable, one rotational and one translational DOF and a gripper have to be added at the end point of the arm.

VII. Conclusions

This paper presents a design for a natural moving robotic arm that uses mechanical resonance to move more energy efficiently. We can conclude that:

- The resonant mechanism as presented makes that the system saves 56% energy per stroke in simulation.
- It does this while still being practical applicable, because it can stand still in a range of angles around its operational positions without consuming energy.
- In prototype experiments we confirmed that the system saves energy, for a one-DOF as well as for a two-DOF setup. The practical energy reduction is less than the theoritical value, warranting further development.

Acknowledgement

The authors would like to thank G. Liqui Lung for helping with the electronical work and J. van Frankenhuyzen for his tips on the mechanical design.

References

[1] A. Dietmar and A. Verl, *A generic energy consumption model for decision making and energy efficiency optimisation in manufacturing.* , International Journal of Sustainable Engineering, 2009. Vol2. No 2: p. 123-133.

[2] Eurostat. *Statistics by Theme.* Available from: http://epp.eurostat.ec.europa.eu/portal/page/portal/statistics/themes.

[3] T. Akinfiev, R. Fernandez, M. Armada, *Nontraditional drives for walking robots.* 8th International Conference on Climbing and Walking Robots and the Support Technologies for Mobile Machines. 2005. Clawar: Springer.

[4] G.J. Grez Joseph, *Method for tuning a spring element used in a resonant driving system for an appliance which includes a work piece*, K.P. Electronics, Editor. 2010: The Netherlands.

[5] M.R. Ribeiro, *Arrangement and Process for mounting a resonant spring in a refrigeration compressor.* 2010: US.

[6] S.H. Klawuhn Manfred, *Oscillating drive for small electrical apparatuses*, B. AG, Editor. 1983: Germany.

[7] S.H. Collins, A. Ruina, R.L. Tedrake, M. Wisse, *Efficient bipedal robots based on passive-dynamic walkers.* Science, 2005. 307: p. 1082-1058.

[8] M.M. Williamson, *Neural control of rythmic arm movements.* Neural networks, 1998. V11(7-8): p. 1379-1394.

[9] M.M. Williamson, *Rhythmic robot arm control using oscillators*, IEEE International conference on Intelligent Robots and Systems. 1998: Victoria, B.C. Canada.

[10] M.M. Williamson, *Robot Arm Control Exploiting Natural Dynamics*, Electrical Engineering and Computer Science. 1999, MIT.
[11] M.M. Williamson, *Designing Rhythmic Motions using Neural Oscillators*, IEEE International conference on Intelligent Robots and Systems. 1999. p. 494-500.
[12] T. Akinfiev, *Resonance drive*, M.P.O. Stankostroitelny, Editor. 1992: Russia.
[13] T. Akinfiev, *Resonance Mechanical hand*, I. mashinoveeniya, Editor. 1985: Russia.
[14] T. Akinfiev, *Resonance Robot*, I.M.I.A.B. Rizh Z Promy Robotov, Editor. 1992: Russia.
[15] T. Akinfiev, V.I. Babitsky, V.S. Kondratiev, V.F. Yurchenkov, *High speed resonant manipulator.* Machine tools and tools. Vol. 2.
[16] V.I. Babitsky, A.V. Shipilov, *Resonant Robotic Systems.* 2003: Springer-Verlag Berlin Heidelberg New York.
[17] B.I. Belov Vladimir, *Resonance Manipulator Modulus*, Editor. 1992: Russia.
[18] M. Sergej, *Resonance Robot*, Editor. 1990: Russia.
[19] P.A. Serov Evgenij, *Resonance Manipulator*, P.O. Rostselmash, Editor. 1990: Russia.
[20] G. Vladimir, *Resonance drive*, V.N.p.o.m. tekhn, Editor. 1990: Russia.